Biocatalytically Templated Synthesis of Titanium Dioxide

Jan L. Sumerel, Wenjun Yang, David Kisailus, James C. Weaver, Joon Hwan Choi, and Daniel E. Morse*

Institute for Collaborative Biotechnologies, Biomolecular Science and Engineering Program, California NanoSystems Institute, and the Materials Research Laboratory, University of California, Santa Barbara, California 93106-9610

Received March 5, 2003. Revised Manuscript Received July 8, 2003

Silicatein, an enzymatic biocatalyst purified from the glassy skeletal elements of a marine sponge, and previously shown capable of catalyzing and structurally directing the hydrolysis and polycondensation of silicon alkoxides to yield silica and silsesquioxanes at low temperature and pressure and neutral pH, is shown to be capable of catalyzing and templating the hydrolysis and subsequent polycondensation of a water-stable alkoxide-like conjugate of titanium to form titanium dioxide. The structure and behavior of the TiO_2 formed through this biocatalytic route, including thermally induced crystal grain growth and phase transformation from anatase to rutile, differ from those of TiO_2 formed from the same precursor via alkali catalysis or thermal pyrolysis. This enzymatic route affords a path to templated synthesis that avoids the high temperatures and extremes of pH typically required for synthesis of metallo-oxanes from the corresponding alkoxide-like precursors, and thus provides access to a new and potentially useful parameter space of structures and properties. The proteins may also be nanoscopically structure-directing, as evidenced by the formation of nanocrystallites of anatase, a polymorph usually formed at much higher temperatures. The summation of weak interactions between the protein and mineral may induce this stabilization and thus may afford a new level of nanostructural control, with associated enhancement of selected performance properties.

Introduction

The molecular mechanisms underlying the biological synthesis of nanostructured mineral−organic composites have long been recognized to offer exciting prospects for materials science.[1−10] In addition to their benign synthesis conditions (including neutral pH, low temperature, low pressure, and the absence of caustic chemicals), these mechanisms often yield a precision of nanostructural control not yet achievable in anthropogenic syntheses. We show here that one such mechanism, normally involved in the biological silica production, can be applied directly to the templated synthesis of the nonbiological material titanium dioxide.

Investigation of the mechanisms governing the biological synthesis of silica structures in a marine sponge (the temperate Eastern Pacific *Tethya aurantia*) led to the surprising discovery that this process may be mediated, in part, by a family of catalytically active, structure-directing enzymes.[8−15] Silica needlelike skeletal elements (spicules) made by *T. aurantia* each contain a central proteinaceous axial filament that spatially directs the deposition of silica along its entire length. These protein filaments are predominantly composed of three highly similar subunits called silicateins (for ***silica*** pro***teins***). Molecular cloning and sequence analysis of the most abundant protein (silicatein α) revealed the surprising fact that this protein belonged to a well-known superfamily of proteolytic and

* To whom correspondence should be addressed. Phone: (805)893-8982. Fax: 805-893-4724. E-mail: d_morse@lifesci.ucsb.edu.

(1) Heuer, A. H.; Fink, D. J.; Laraia, V. J.; Arias, J. L.; Calvert, P. D.; Kendall, K.; Messing, G. L.; Blackwell, J.; Rieke, P. C.; Thompson, D. H.; Wheeler, A. P.; Veis, A.; Caplan, A. I. *Science* **1992**, *255*, 1098.
(2) Mann, S. *Nature* **1993**, *365*, 499.
(3) Sarikaya, M., Aksay, I. A., Eds. *Biomimetics: Design and Processing of Materials*; American Institute of Physics Press: Williston, VT, 1995.
(4) Hoch, H. C., Jelinski, L. W., Craighead, H. G., Eds. *Nanofabrication and Biosystems*; Cambridge University Press: Cambridge, U.K., 1996.
(5) Ball, P. *Made to Measure*; Princeton University Press: Princeton, NJ, 1997.
(6) Benyus, J. M. *Biomimicry;* William Morrow and Co.: New York, 1997.
(7) Timp, G., Ed. *Nanotechnology;* Springer-Verlag: New York, 1998.
(8) Morse, D. E. *Trends Biotechnol.* **1999**, *17*, 230.
(9) Morse, D. E. *The Chemistry of Organic Silicon Compounds*, *Vol. 3*; Rappoport, Z., Apeloig, Y., Eds.; John Wiley & Sons: New York, 2001.
(10) Sumerel, J. L.; Morse, D. E. *Silicon Biomineralization: Biology − Biochemistry − Molecular Biology − Biotechnology*; John Wiley and Sons: New York, 2003, in press.
(11) Shimizu, K.; Cha, J.; Stucky, G. D.; Morse, D. E. *Proc. Natl. Acad. Sci. U.S.A.* **1998**, *95*, 6234.
(12) Cha, J. N.; Shimizu, K.; Zhou, Y.; Christiansen, S. C.; Chmelka, B. F.; Stucky, G. D.; Morse, D. E. *Proc. Natl. Acad. Sci. U.S.A.* **1999**, *96*, 361.
(13) Cha, J. N.; Stucky, G. D.; Morse, D. E.; Deming, T. J. *Nature* **2000**, *403*, 289.
(14) Zhou, Y.; Shimizu, K.; Cha, J. N.; Stucky, G. D.; Morse, D. E. *Angew. Chem. Intl. Ed.* **1999**, *38*, 779.
(15) Weaver, J. C.; Morse, D. E. *Microsc. Res. Tech.*, in press.

10.1021/cm030254u CCC: $25.00
Published on Web 11/15/2003

hydrolytic enzymes.[11] On the basis of this finding, these intact filaments, and their constituent monomers obtained from disaggregation of the filaments or produced from recombinant DNA templates cloned in bacteria, were shown in vitro to catalyze the hydrolysis and structurally direct the polycondensation of silicon alkoxide precursors to form silica and polysilsesquioxanes at neutral pH.[12] Genetic engineering by site-directed mutagenesis confirmed the essential participation of the serine, histidine, and asparagine residues of the catalytic triad in the in vitro polymerization of silica.[14] Predictive synthesis of biomimetic diblock copolypeptides based on the deduced catalytic constituents of the native silicateins yields catalytically active molecules that exhibit both silica-polymerizing and structure-directing capabilities.[13] We show here that the silicatein filaments also can be used to catalyze the hydrolysis and subsequent polycondensation of a water-stable alkoxide-like conjugate of titanium to yield titanium dioxide at neutral pH. Thermal annealing of the initially amorphous/partially nanocrystalline TiO_2 progressively yields nanocrystals of anatase and rutile.

Materials and Methods

Isolation of Silicatein Filaments. Specimens of the sponge *Tethya aurantia* were collected at 17-M depth off Santa Barbara, California (latitude 34°25.331′N, longitude 119°57,142′W). Sponges were washed with seawater, broken into ca. 1-cm cubes, and bleached with sodium hypochlorite solution until all of the cellular material had been destroyed. The spicules were washed with (Millipore) Milli-Q-purified (MQ) water 5× and then air-dried. Dry spicules were cleaned with concentrated HNO_3/H_2SO_4 (1:4) overnight. Acid-insoluble material (consisting entirely of the cleaned silica spicules) was rinsed with water to neutrality. After air-drying, this material was treated with 2.5 M HF for 2.5 h to dissolve the silica and release the occluded axial filaments. The filaments were washed in 40 mL of MQ water 3× before dialysis. The protein filaments were dialyzed against 8 L of MQ water at 4 °C for 8 h per dialysis, and the outer solution was changed 5×. The dialysate was either settled by gravity or collected by centrifugation in a Sorvall RC 5C centrifuge (DuPont, Wilmington, DE) at 10 000*g* for 20 min at 4 °C or lyophilized until dry.

Silicatein Denaturation. Approximately 50-μg aliquots of lyophilized silicatein filaments were placed in small plastic centrifuge vials (500 μL) filled with water. A small hole was placed in the top of each sealed vial to avoid pressure buildup during heating. The vials were then placed in a heated water bath (95 °C) for 1 h. After thermal denaturation, the filaments were immediately used (as negative controls) in subsequent TiO_2 synthesis experiments.

Silicatein-Catalyzed Synthesis of TiO_2. Silicatein filaments in water were added to 1.6-mL polyethylene centrifuge tubes containing an aqueous solution of titanium(IV) bis-(ammonium lactato)-dihydroxide (Ti[BALDH], from Aldrich), a water-stable alkoxide-like conjugate of titanium. The filaments then were mixed with the precursor solution by pipetting for 2 min and immediately placed on a rotator (Labnet, Woodbridge, NJ). The filament−precursor suspensions were mixed on the mill at 50 rpm for 24 h at 20 °C. Following this reaction period, the samples were centrifuged at 5000 rpm for 20 min. Residual precursor in the supernatant was separated from the solid product by pipetting. Unreacted precursor was extracted by three successive cycles of mixing with water followed by centrifugation, and the remaining solid product was dried by evaporation in an oven at 37 °C for 24 h. Parallel experiments were conducted with native and denatured filaments.

Preparation of TiO_2 by Alkali-Catalysis and by Thermal Decomposition of the Precursor. To compare the crystallization behavior of TiO_2 derived by silicatein-mediated catalysis to TiO_2 made without the participation of the protein, powder samples of TiO_2 were prepared by alkali-catalyzed hydrolysis and by pyrolysis of Ti[BALDH].

Base-catalyzed (BC) synthesis of TiO_2 was accomplished by placing 1 g of 50% (w/w) Ti[BALDH], 15 g of water, and 1 g of concentrated (∼28% w/w) ammonium hydroxide (NH_4OH) into a 45-mL Teflon-lined hydrothermal vessel (Parr Instruments, Moline, IL). The vessel was then sealed and subsequently heated to 150 °C for 12 h. After the vessel cooled, the powder was removed and washed 5× with MQ water. The resulting powder was used for further heat treatments.

Pyrolysis of the precursor was performed with 3.0 g of Ti[BALDH] in an alumina boat placed in a quartz Schlenk tube. The tube was sealed and heated (20 °C/min) in flowing air (50 cm^3/minute) to 600 °C for 1 h. The resulting powder was used for further heat treatment studies.

Thermal Annealing and Analyses of TiO_2 Crystallization. Dried product formed by silicatein-mediated catalysis was ground in an agate mortar to a fine powder. Samples then were heated in air on a temperature-controlled-stage X-ray diffractometer (Siemens D5005) and analyzed (Cu Kα radiation; $2\theta = 3-40°$) successively at 100° increments from 27 to 927 °C.

Samples (ca. 100 mg) of alkali-catalyzed or directly pyrolyzed precursor were heated in alumina boats in quartz Schlenk tubes. The tubes were sealed and heated (20 °C/min) in flowing air (50 cm^3/min) to temperatures between 600 and 1000 °C for 1 h. Approximately 25 mg of these samples was then ground to a fine powder, placed on single-crystal (100) silicon wafers (Materials Technology Incorporated; Richmond, CA), and characterized by X-ray diffraction (Phillips X'Pert; Amsterdam, The Netherlands) using a $2\theta - \omega$ scan from 20 to 60° (0.02°/step, 5 s/step; slit sizes of $^1/_4$, $^1/_2$, $^1/_4$, and 0.2 mm from source to detector, respectively).

Average crystal diameters of anatase and rutile powders were determined (for nanocrystals assumed to be approximately spherical) by measurement of the full width at half-maximum (fwhm) of the (101) anatase and (110) rutile planes, respectively, and applying these to the Scherrer formula[16] assuming that the crystal diameter is equal to the X-ray structural coherence length. Line broadening due to instrumental effects was removed prior to crystallite diameter calculations.[17]

Scanning Electron Microscopy and Energy Dispersive Spectroscopy. Surface features of TiO_2 precursor-derived powders and coated silicatein filaments were imaged by a cold cathode field emission scanning electron microscope (SEM; JEOL JSM 6300F, Peabody, MA) equipped with an energy dispersive spectrometer. Specimens were mounted on conductive carbon adhesive tabs (Ted Pella, Inc., Redding, CA) and examined (at 5 or 10 kV) either uncoated (for EDS analysis) or after gold/palladium sputter-coating (for imaging). Energy dispersive spectrometry (EDS, Oxford Instruments, Palo Alto, CA) was performed in conjunction with SEM to qualitatively determine elemental composition of the samples.

A variation of the procedure for alkali-catalyzed synthesis described above was used, and the resulting material was examined by SEM. Powders were prepared by mixing 1 g of 50% (w/w) Ti[BALDH] with 1 mL of 1 N NaOH, collected by centrifugation, washed repeatedly with water, and then dried and imaged as described above.

X-ray Photoelectron Spectroscopy. Quantitative elemental analyses of TiO_2 surfaces were determined by X-ray photoelectron spectroscopy (XPS, Kratos Axis Ultra spectrophotometer). The binding energies (and hence, bonding states) of the titanium atoms in a 15 × 15 μm area of each sample were determined by examination of the intensity, shape, and energy of the Ti 2p peak. Peak energies were normalized to the carbon 1s peak at 285 eV.

(16) Brinker, J. C.; Scherer, G. W. *Sol−Gel Science*; Academic Press: New York, 1990.

(17) Klug, H. P.; Alexander, L. E. *X-ray Diffraction Procedures;* Wiley: New York, 1974.

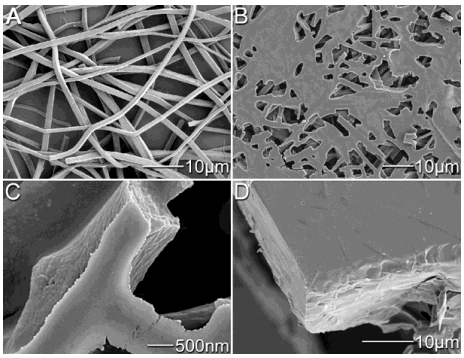

Figure 1. Scanning electron micrographs comparing TiO_2 products formed from Ti[BALDH] by catalysis with the purified silicatein filaments: heat-denatured filaments after reaction with the TiO_2 precursor (A); native filaments after the same reaction conditions (B); enlargement of figure B illustrating the apparent templating activity of the filaments (C); at very high filament densities, TiO_2 polycondensation continues to generate a solid inorganic/organic composite of protein filaments encased in titanium dioxide (D).

Transmission Electron Microscopy. Coated filaments were examined with a transmission electron microscope (TEM, JEOL 2000FX, Tokyo) to characterize the coatings in cross-section and to obtain electron diffraction patterns. Specimens were prepared by pipetting a small amount (~20 μL) of filament suspension (in water) onto conductive holey carbon copper grids (Ted Pella, Inc., Redding, CA). The grids were then dried at 40 °C for 5 min. Samples were imaged (200 kV) at magnifications from 20 000 to 200 000×, and selected area electron diffraction patterns (SADP) were acquired at a camera distance of 83 cm.

Fluorescence Spectroscopy. Photoluminescence studies of coated filaments were conducted using a spectrofluorometer (FluoroMax-EMAX-2; Jobin Yvon-Spec Instruments Inc., Edison, NJ) with excitation at 280 nm.

Results

Silicatein filaments at neutral pH and 20 °C catalyzed the hydrolysis and polycondensation of titanium(IV) bis-(ammonium lactato)-dihydroxide, forming an extended metallo-oxane subsequently identified as amorphous/nanocrystalline titanium dioxide (Figure 1B−D). After initially following the contours of the silicatein filaments, at high filament densities, TiO_2 polycondensation continued to generate a solid inorganic/organic composite of protein filaments encased in amorphous titanium dioxide (Figure 1D). In contrast, Ti[BALDH] mixed with heat-denatured silicatein filaments yielded neither a precipitate nor a coating on the filament surfaces after 24 h (Figure 1A), indicating that the activity of the silicatein filaments was dependent upon the integrity of the 3-dimensional structure of the protein monomers (cf. ref 12).

On the basis of the broadness and location of peaks (or lack thereof due to the inability or insufficient number of small crystallites to coherently diffract X-rays), X-ray diffraction analyses (data not shown) revealed that both powder and coated filament products were largely amorphous TiO_2. Elemental composition of these products was confirmed by energy-dispersive spectroscopy (EDS), indicating that the specimen shown in Figure 1D consisted of titanium, oxygen, and carbon (Figure 2). Further examination of the coated filaments by transmission electron microscopy (TEM) showed that the filaments were coated with regions of both amorphous and nanocrystalline titanium dioxide (Figure 3). A selected area diffraction pattern (SADP) obtained from the coating close to the filament surface (lower image, Figure 3) exhibited relatively sharp rings with spots having *d* spacings of 3.5, 2.4, and 1.9 Å. The relative intensities of the diffraction rings and their corresponding *d* spacing values matched the 3 most intense values for nanocrystalline TiO_2 (anatase phase, JCPDS 84-1286). The corresponding lattice planes for the aforementioned *d* spacings seen in the SADP are (101), (004), and (200), respectively. Regions observed away from the interface of the filament and coating were found to be amorphous as observed by selected area diffraction (figure not shown).

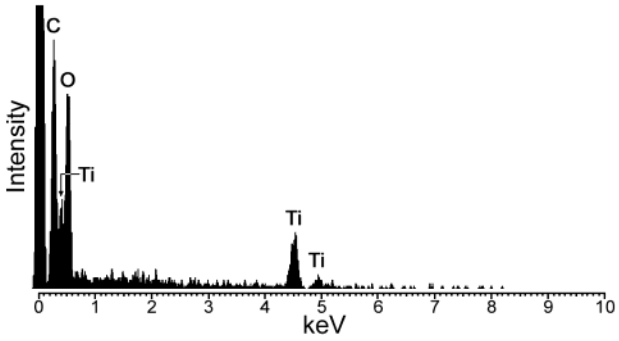

Figure 2. Energy dispersive spectrum of TiO_2−silicatein filament composite. Analysis of the sample illustrated in Figure 1C, as described in the text.

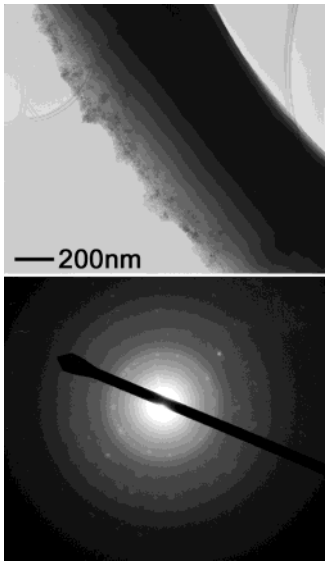

Figure 3. Transmission electron micrograph of TiO_2-coated filaments formed from reaction with Ti[BALDH]; selected area diffraction pattern obtained near the filament-coating interface (lower image).

The oxidation states of titanium in the filament coatings were analyzed by X-ray photoelectron spectroscopy (XPS, Figure 4). Quantitative analysis of the protein−inorganic composite revealed the presence of 33% oxygen, 5% titanium, 52% carbon, and 3% nitrogen. Further analysis of the Ti 2p 3/2 and 1/2 orbitals demonstrated that 71% of the titanium was in the +4 state (peaks A and C), while 29% is in the +3 state (peaks B and D).

Photoluminescence spectra (Figure 5) revealed that the TiO_2/protein composite exhibited a broad luminescence peak between 450 and 550 nm (2.76−2.26 eV)

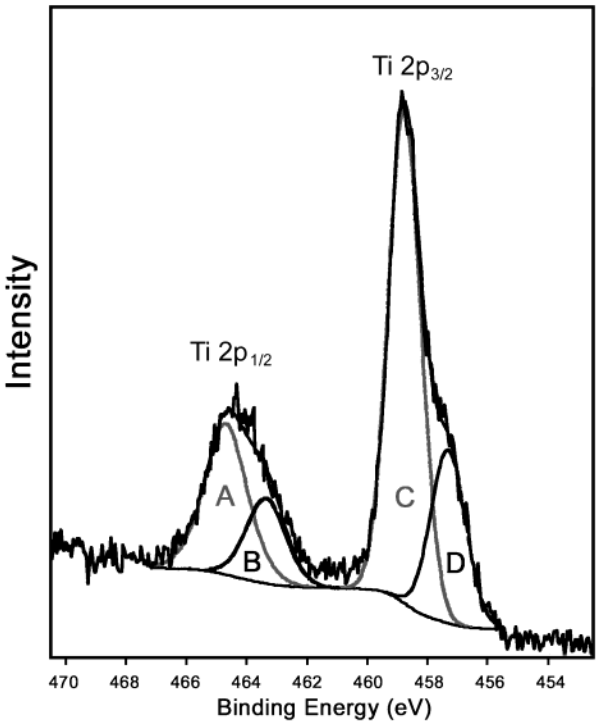

Figure 4. X-ray photoelectron spectrum of TiO_2−silicatein filament composite. The high-resolution spectrum of the Ti 2p orbital indicates oxidation states of +4 (peaks A and C) and +3 (peaks B and D). The spectrum is normalized to the carbon 1s peak (285 eV).

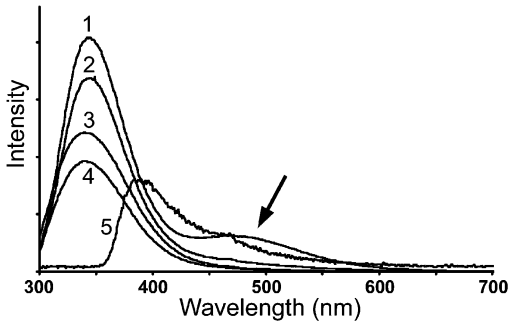

Figure 5. Photoluminescence of TiO_2−silicatein filament composite after excitation at 280 nm: curve 1, native filament after reaction with Ti[BALDH], (the secondary peak, indicated by the arrow, is indicative of TiO2 emission); 2, denatured filament after exposure to Ti[BALDH]; 3, native filament alone; 4, denatured filament alone; and 5, Ti[BALDH] alone.

with an emission maximum at ca. 475 nm (2.61 eV) when excited at 280 nm. Control spectra from the protein filaments alone and from thermally denatured (inactive) filaments reacted with Ti[BALDH] exhibited identical spectra without the broad peak from 450 to 550 nm. Photoluminescence of rutile and anatase TiO_2 crystalline powder standards exhibited luminescence peaks at 2.82 and 2.92 eV, respectively (not shown).

Controlled heating monitored by X-ray diffraction was used to analyze the progressive conversion of the amorphous/nanocrystalline TiO_2 in the initial protein-catalyzed product to the nanocrystalline anatase and rutile phases (Figure 6). Heating the material in 100 °C increments produced a distinct crystalline anatase peak ($2\theta = 25.25°$) at ca. 427 °C. The rutile phase was not detectable until samples were heated between 827 °C and 927 °C ($2\theta = 27.25°$). Additional experiments in which samples were heated in a quartz Schlenk tube and subsequently X-rayed from $2\theta = 20-40°$ narrowed the anatase-to-rutile transition temperature to ca. 850 °C (Table 1). The broad diffraction peaks observed (Figure 6) are characteristic of the nanocrystalline nature of the samples. Debye−Scherrer analyses of peak-widths were used to estimate the average crystallite diameters (Table 1) with the assumption that the crystal diameter is equal to the X-ray structural coherence length. These data demonstrate that when silicatein filaments are used as the catalyst for titanium dioxide synthesis from the Ti[BALDH] precursor, the transition to rutile does not occur until 850 °C (97% rutile, 3% anatase). However, base-catalyzed synthesis from this precursor reduced the anatase-to-rutile transition temperature to 700 °C. When thermally decomposed (noncatalyzed) Ti[BALDH] was heat treated, the transition from anatase to rutile began at 800 °C. Thus, the transition to rutile is delayed in TiO_2 on the filament surface. As expected, crystal diameters range from ca. 2 nm when formed by silicatein-mediated catalysis at relatively low temperatures (e.g., 400 °C) to ca. 50 nm when formed at higher annealing temperatures (e.g., 850 °C).

Discussion

Catalysis of TiO_2 Synthesis from the Water-Stable Alkoxide-Like Precursor. Previous studies had revealed that siliceous sponge-spicule axial filaments and their constituent silicatein monomers (either purified from the sponge biosilica, or produced from recombinant DNA templates cloned in bacteria) catalyze and structurally direct the hydrolysis and subsequent polycondensation of silicon and organosilicon alkoxides, at neutral pH and low temperature, to form the corresponding SiO_2 and silsesquioxanes, respectively[8−10,12,14,15]. Genetic engineering was used to generate a series of substituted silicateins, thereby allowing confirmation of the identities of the critical amino acid side chains in the postulated mechanism of catalysis.[14] This identification was further confirmed by the predictive synthesis of a family of self-assembling diblock copolypeptides incorporating functionalities which mimicked the activities of the native silicatein, thereby acting as "biomimetic", structure-directing catalysts.[13]

As shown here, this catalytic activity of the silicatein filaments extends to the hydrolysis and polycondensation of Ti(BALDH), a water-stable alkoxide of titanium, leading to the synthesis of amorphous/nanocrystalline TiO_2 at neutral pH and room temperature. In the absence of silicatein, this synthesis normally requires either pyrolytic decomposition of the precursor or alkali catalysis. When the silicatein proteins are first subjected to thermal denaturation (at 95 °C) they fail to react catalytically with the titanium precursor, proving that this specific activity is dependent upon the integrity of the protein's 3-dimensional structure (as is the case for its activity with silicon alkoxides; cf. refs 12 and 14). Although the mechanism of the catalytic reaction between silicatein and Ti[BALDH] has not yet been examined, in the case of the silicon alkoxides such as tetraethyl orthosilicate (TEOS), the evidence cited above supports the role of a specific serine−histidine pair in the enzyme's active site. Hydrogen bonding between the

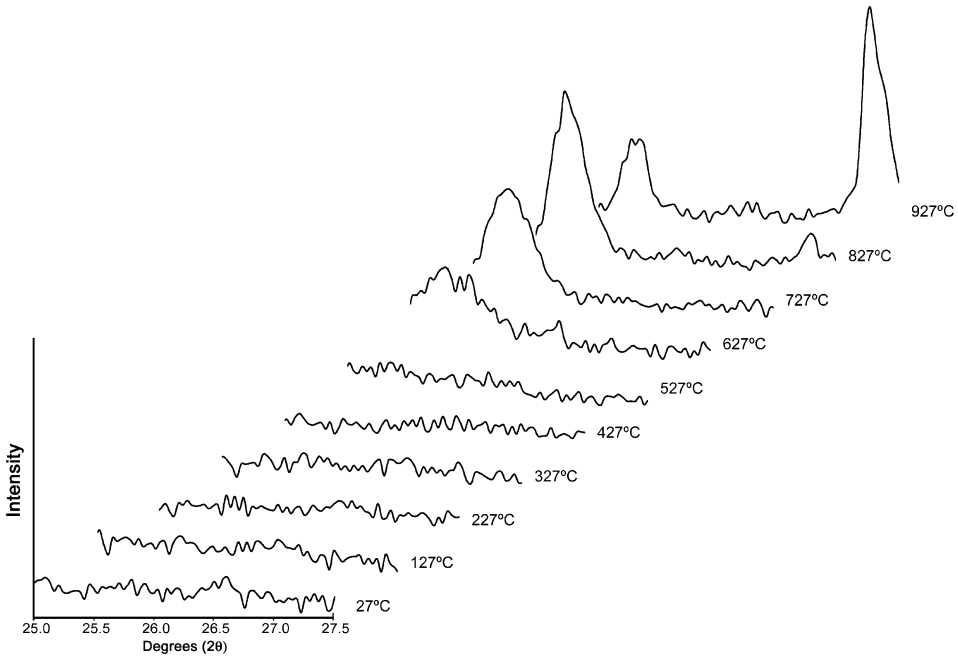

Figure 6. X-ray diffraction of TiO_2 powders formed from Ti[BALDH] by reaction with silicatein filaments as a function of the temperature of thermal annealing.

Table 1. Crystallite Diameters and Phases of TiO_2 Powders Derived from Ti[BALDH] as a Function of Synthesis Catalyst and Temperature of Thermal Annealing

	thermal catalysis		alkali catalysis		silicatein catalysis	
temp. (°C)	diam. (nm)	phase (%)[a]	diam. (nm)	phase (%)[a]	diam. (nm)	phase (%)[a]
400					2.0	100% A
600	4.5	100% A	13.5	100% A	9.1	100% A
700			22.5	98% A; 2% R		
800	31.6	9% A 91% R	39.0	43% A 57% R	19.1	100% A
850	44.8	100% R	53.1	100% R	53.4	3% A; 97% R

[a] A = anatase; R = rutile.

hydroxyl side chain of the serine and the imidazole side chain of the histidine apparently increases the nucleophilicity of the serine oxygen, facilitating its attack on the silicon in silicon alkoxides to form a transitory Si−O bond with the protein to initiate hydrolysis of the alkoxide at neutral pH.[8,9,12,14] We suggest that a similar mechanism may account for the silicatein-mediated catalysis of TiO_2 synthesis from the water-stable alkoxide-like precursor described here.

Templated Synthesis and the Surface Morphology of TiO_2. There are obvious morphological differences between the TiO_2 surfaces resulting from the silicatein- and base-catalyzed syntheses (figure not shown). Silicatein-mediated catalysis yields a product that is much smoother than that of the TiO_2 formed by base-catalysis. Both this difference in roughness and the apparent templating-like activity of the silicatein filaments (cf. Figure 1) may be directly related to the nucleation mechanism occurring during the growth of TiO_2. In silicatein filament-directed growth, there apparently are numerous nucleation sites (e.g., clusters of contiguous −OH side chains on the silicatein protein; cf. ref 11) upon which the newly formed TiO_6 octahedra could feasibly condense. Such structural features of the filaments may enhance the Gibbs free energy barrier differential between heterogeneous nucleation (on the filament surfaces) and the intrinsically higher barrier for homogeneous nucleation (e.g., via base-catalyzed precipitation from solution). By offering favorable surfaces on which nuclei can form, the silicatein filaments may act initially as a template and stabilize smaller nuclei (with lower surface roughness) than formed by homogeneous nucleation. The potential for a summation of weak interactions (i.e., hydrogen bonding and van der Waals forces) at the interface between the filament surface and the crystallizing mineral may stabilize the anatase polymorph of TiO_2 that normally is formed only at much higher temperatures.

TiO_2 Phase Evolution and Crystal Growth. Characterization of the room-temperature synthesis products indicated that the TiO_2 material deposited on the silicatein filaments revealed regions of both amorphous and nanocrystalline natures. Selected area electron diffraction patterns obtained by TEM near the silicatein−TiO_2 interface (Figure 3) reveals sharp rings with diffraction spots having *d* spacings that match the nanocrystalline anatase phase of TiO_2 within ∼1% of the values reported for standards. Other regions investigated by selected area diffraction showed faint, diffuse rings, indicating that the TiO_2 is composed of both nanocrystalline and amorphous material (hereafter referred to as amorphous/nanocrystalline). The small size and ratio to total sample volume of these crystallites made them difficult to detect by standard X-ray diffraction methods. Additional experiments were done to show that electron beam exposure from the TEM did not cause the transformation from amorphous to crystalline TiO_2. The beam was placed on amorphous regions of the specimen for 1, 5, 15, and 30 min. Subsequent analysis by selected area diffraction showed that the irradiated TiO_2 remained amorphous after each exposure.

Transformation from anatase to rutile occurred at significantly different temperatures for the powders formed via the three different synthesis routes. The TiO_2 prepared by alkaline catalysis began to transform at a temperature of ca. 700 °C (2% rutile), whereas the product obtained from thermal decomposition of the Ti-[BALDH] did not start to transform until 800 °C. Interestingly, this transformation was delayed to the highest temperature (825 °C) for the TiO_2 produced by silicatein-mediated catalysis (Figure 6). The range of temperatures over which the complete transformation occurred also differed among the three samples. Complete transformation from anatase to rutile occurred over a broad temperature range (∂T = ca. 150 °C) for the material derived from alkali catalysis, whereas the other two samples transformed over a much narrower range (∂T = ca. 50 °C).

Several factors can inhibit grain growth and shift this transformation to higher temperatures. For example, (1) the presence of carbon (from the underlying filament or from unhydrolyzed ligands) or other impurities admixed with the TiO_2 can interrupt not only the crystallization of the amorphous material,[18,19] but also slow the diffusion of ions necessary for rearrangement and grain growth. In addition, (2) strain energies imposed on the crystal surfaces (e.g., through in-plane alignment and/or interactions with heterogeneous nucleating or templating surfaces) also can impede phase transformations. Additional factors that may contribute to the higher transition temperature and slower grain growth seen in the material produced via silicatein catalysis include (3) the possible trapping within the TiO_2 coating of volatilized organic material from the silicatein filaments themselves (which become pyrolyzed at temperatures near 600 °C) or carbon from incompletely hydrolyzed precursor.

Photoluminescence. Physical characterization revealed that the low-temperature (25 °C) product of silicatein catalysis consisted of a mixture of amorphous TiO_2 and nanocrystalline anatase. This material exhibited a broad luminescence peak between 450 and 550 nm (2.76−2.26 eV) with a maximum at ca. 475 nm (2.61 eV). This luminescence is ca. 0.31 eV lower than the 2.92 eV band-edge of the broad luminescence exhibited by anatase powder standards. The shift in luminescence is probably due to impurities of carbon and oxygen contributed by residual organic ligands from the Ti-[BALDH] precursor that were not completely removed by hydrolysis and condensation catalyzed by the silicatein filaments. Such impurities can act as acceptor−donor pairs, reducing the band gap of the TiO_2. Another possible contributor to this energy shift would be vacancies in the TiO_2. [20] Such vacancies have been found to cause shifts in luminescence in other wide band gap materials (e.g., GaN).[21]

XPS analysis revealed the presence of both +3 and +4 Ti, strongly supporting the suggestion that the charge balance in the TiO_2 product is maintained by the formation of vacancies.[22,23] The presence of a distinct shoulder in the Ti 2p 1/2 and 3/2 peaks[24] was clearly observed in oxygen-deficient TiO_2 by high-resolution XPS (Figure 4) and subsequently identified as Ti 3+. Differential charging as a source of the observed shoulder was excluded by the discrete nature of this shoulder (as opposed to peak broadening) and the lack of symmetry relative to the overall Ti 2p 1/2 and 3/2 peaks.[22]

Potential Significance. The results presented here demonstrate that silicatein, an enzymatic biocatalyst previously shown capable of catalyzing and structurally directing the hydrolysis and polycondensation of silicon alkoxides at neutral pH,[10,12,14,15] also is capable of catalyzing and templating the hydrolysis and subsequent polycondensation of a water-stable titanium alkoxide-like conjugate to form titanium dioxide. The properties of the TiO_2 formed through this biocatalytic route differ from those of TiO_2 formed from the same precursor via alkali catalysis or thermal pyrolysis. Although enzymatic biocatalysis has long been used to produce compounds and materials based on carbon, these observations are the first of which we are aware to extend this approach to valuable inorganics such as TiO_2. As demonstrated here, this enzymatic route affords a path to templated synthesis that avoids the high temperatures or extremes of pH typically required for synthesis of the metallo-oxanes from the corresponding alkoxide (and alkoxide-like) precursors (cf. ref 25 and thus provides access to a new and potentially useful parameter space of structures and properties. As illustrated here, these conditions also protect and preserve the integrity of complex biochemical structures (in the example shown here, the silicatein filaments themselves) on which the metallo-oxanes can be deposited, and with which they can thus be integrally fabricated. The templating and potential structure-directing activity of the proteins may afford a new level of nanostructural control, with associated enhancement of selected performance properties.

Acknowledgment. We thank Jason Rouse for first bringing to our attention the water-stability of the titanium lactate complex used in this study. This work was supported by grants from the U.S. Department of Energy (DE-FG03-02ER46006), NASA (NAG1-01-003), the NOAA National Sea Grant College Program, U.S. Department of Commerce (NA36RG0537, Project R/MP-92) through the California Sea Grant College System, and the MRSEC Program of the National Science Foundation under award DMR-96-32716 to the UCSB Materials Research Laboratory. The U.S. Government is authorized to reproduce and distribute copies for governmental purposes.

CM030254U

(18) Gruy, F.; Pijolat, M. *J. Am. Ceram. Soc.* **1992**, *75*, 663.
(19) Hahn, H.; Logas, J.; Averack, R. S. *J. Mater. Res.* **1990**, *5*, 609.
(20) Lindan, P. J. D.; Muscat, J.; Bates, S.; Harrison, N. M.; Gillan, M. *Faraday Discuss.* **1997**, *106*, 135.
(21) Hoffmann, A. *Mater. Sci. Eng.* **1997**, *B43*, 185.
(22) Kim, K. W.; Lee, E. H.; Kim, Y. J.; Lee, M. H.; Kim, K. H.; Shin, D. W. *J. Photochem. Photobiol. A: Chem.* **2003**, *159*, 301.
(23) Mouler, J. F.; Stickle, W. F.; Sobol, P. E.; Bomben, K. D. *Handbook of X-ray Photoelectron Spectroscopy*; Physical Electronics, Inc.: Eden Prairie, MN, 1995.
(24) Hebensteit, E. L. D.; Hebenstreit, W.; Diebold, U. *Surf. Sci.* **2000**, *461*, 87.
(25) Rouse, J. H.; Ferguson, G. S. *Adv. Mater.* **2002**, *14*, 151.